ChemPhysMater 1 (2022) 6–16

Contents lists available at ScienceDirect

ChemPhysMater

journal homepage: https://www.keaipublishing.com/en/journals/chemphysmater/

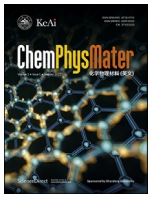

Review Article

Electromagnetic wave manipulation based on few-layer metasurfaces and polyatomic metasurfaces

Shiwang Yu[a], Jiaqi Cheng[a], Zhancheng Li[a,*], Wenwei Liu[a], Hua Cheng[a,*], Jianguo Tian[a], Shuqi Chen[a,b,*]

[a] The Key Laboratory of Weak Light Nonlinear Photonics, Ministry of Education, Renewable Energy Conversion and Storage Center, School of Physics and TEDA Institute of Applied Physics, Nankai University, Tianjin 300071, China
[b] The Collaborative Innovation Center of Extreme Optics, Shanxi University, Taiyuan 030006, China

ARTICLE INFO

Keywords:
EM wave manipulation
Few-layer metasurfaces
Polyatomic metasurfaces
Collective interference

ABSTRACT

Metasurfaces, whose electromagnetic (EM) responses can be artificially designed, are two-dimensional arrays composed of subwavelength nanostructures. Accompanied by various fascinating developments in the past decade, metasurfaces have been proved as a powerful platform for the implementation of EM wave manipulation. However, the planar monoatomic metasurfaces widely used in previous works have limited design freedoms, resulting in some disadvantages for the realization of high-performance and new functional EM wave control. The latest developments show that few-layer metasurfaces and polyatomic metasurfaces are good alternatives to overcome the drawbacks of planar monoatomic metasurfaces and realize high-efficient, multi-band and broadband EM functionalities. They provide additional degrees of design freedom via introducing multilayer layouts or combining multiple meta-atoms into a unit cell respectively. Here, recent advances of few-layer and polyatomic metasurfaces are reviewed. The design strategies, EM properties and main advantages of few-layer metasurfaces and polyatomic metasurfaces are overviewed firstly. Then, few-layer metasurfaces and polyatomic metasurfaces in recent progress for EM wave manipulation are classified and discussed from the viewpoint of their design strategy. At last, an outlook on future development trends and potential applications in these fast-developing research areas is presented.

1. Introduction

Arbitrary manipulation of EM waves is one of the most important tasks in modern optics and photonics, which enables optoelectronic devices with on-demand functionalities [1]. Conventional materials mainly rely on the light propagation and refraction to manipulate EM waves, so their control capabilities are usually limited. Metasurfaces, which consist of subwavelength spaced artificial structures (meta-atoms), emerged as good alternatives to arbitrarily control EM waves [2–7]. By varying the constituent materials, structural parameters and structural symmetry of the meta-atoms in a metasurface, the amplitude, phase, and polarization of EM waves can be freely modified, which lead to single-dimensional and multidimensional manipulations of EM waves [8–13]. Thanks to their prominent wave-manipulation capabilities, metasurfaces with multiple information channels or functionalities are further proposed to realize concurrent tasks [14–17]. So far, metasurfaces for EM wave manipulation are mainly single-layer monoatomic designs. In these designs, the meta-atoms are designed on the surface of a substrate, while every unit cell is composed of one meta-atom. As a simple and fundamental design, planar monoatomic metasurfaces have fewer degrees of design freedom, inducing their limited functionality and controllability [18]. For the purpose of improving the device performance and obtaining kaleidoscopic designs, it is necessary to search for new approaches to increase the design freedoms of metasurfaces.

In chemistry, the polyatomic molecules synthesized by several atoms can have different molecular formulas and spatial configurations, leading to different physical and chemical properties. Predictably, involving multiple meta-atoms into a unit cell will significantly increase the design freedoms of metasurface, which is now attracting more and more attentions from the researchers. Metasurfaces with more than one meta-atom in a unit cell can be classified into two categories, the few-layer metasurfaces and the polyatomic metasurfaces, as shown in Fig. 1. In the unit cell of the former, the multiple meta-atoms are introduced in the direction perpendicular to the surface, while the multiple meta-atoms in

* Corresponding authors at: The Key Laboratory of Weak Light Nonlinear Photonics, Ministry of Education, Renewable Energy Conversion and Storage Center, School of Physics and TEDA Institute of Applied Physics, Nankai University, Tianjin 300071, China.
E-mail addresses: zcli@nankai.edu.cn (Z. Li), hcheng@nankai.edu.cn (H. Cheng), schen@nankai.edu.cn (S. Chen).

https://doi.org/10.1016/j.chphma.2021.09.001
Received 29 July 2021; Received in revised form 30 August 2021; Accepted 4 September 2021
Available online 14 October 2021

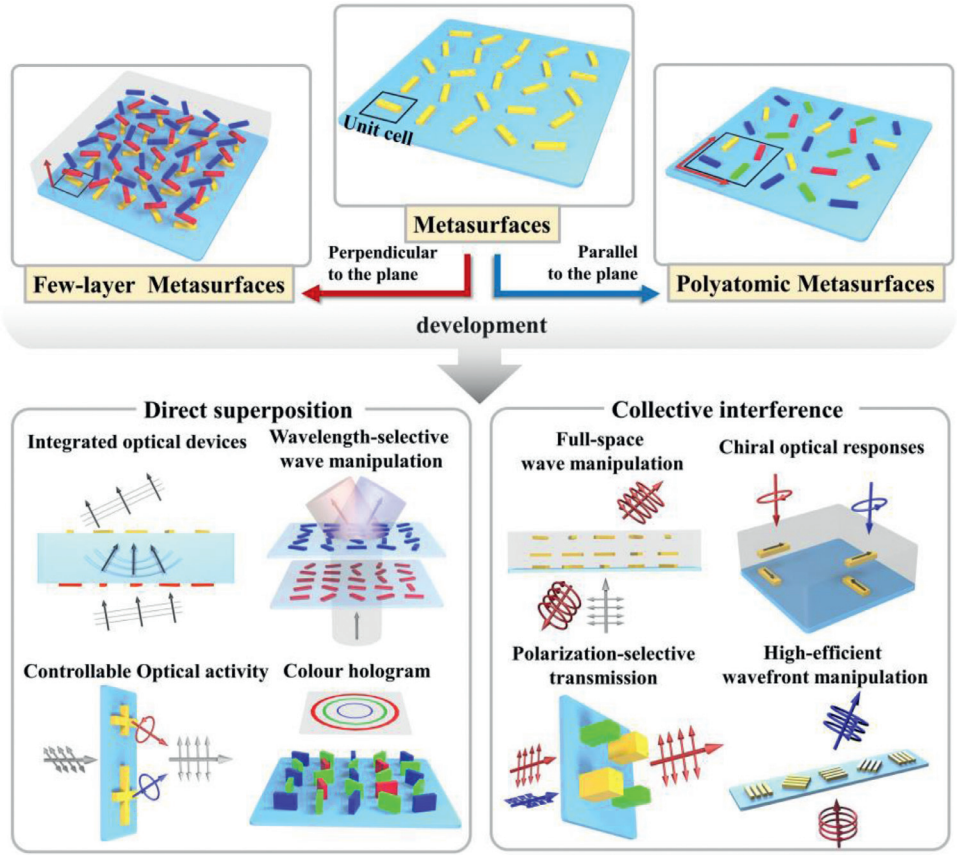

Fig. 1. Conceptions of few-layer metasurfaces and polyatomic metasurfaces and an overview of the EM waves manipulation based on them. Both the few-layer metasurfaces and the polyatomic metasurfaces can be classified into two categories from the viewpoint of their design strategies: the direct superposition strategy and the collective interference strategy. For few-layer metasurfaces and polyatomic metasurfaces designed based on the direct superposition strategy, the resonances of meta-atoms in the unit cell are independently designed and the couplings between the meta-atoms in a unit cell is negligible. On the contrary, for few-layer metasurfaces and polyatomic metasurfaces designed based on the collective interference strategy, the neighbor interaction between the meta-atoms in a unit cell play a decisive role in the EM responses of metasurfaces.

the unit cell of the latter are introduced in the direction parallel to the surface. Therefore, the polyatomic metasurfaces are planar arrays based on super unit cells composed of multiple meta-atoms, which can be fabricated by techniques commonly used for planar monoatomic metasurfaces, such as electron beam lithography and focused ion beam lithography [19]. Few-layer metasurfaces cannot be simply treated as one kind of polyatomic metasurfaces, since the light-matter interaction mechanisms in few-layer metasurfaces are different from the ones in planar metasurface, part of which is inexistent in planar metasurfaces (such as the Fabry-Perot interference and the waveguide effect) [20]. Few-layer metasurfaces are always composed of several layers of meta-atoms embedded into a transparent substrate (for example, SU-8 photoresist and fused silica are widely used as substrate in the visible and near-infrared regime), which can be fabricated by well-established top-down nano fabrication techniques, such as the top-down electron beam lithography [21,22]. Since the fabrication techniques of few-layer and polyatomic metasurfaces are similar to those of the planar monoatomic ones, optical materials widely used as the constituent materials of the planar monoatomic metasurfaces can also be used in the design of few-layer and polyatomic metasurfaces. Since every meta-atom in the unit cell can be independently designed, few-layer and polyatomic metasurfaces offer more design freedoms compared with single-layer monoatomic metasurfaces, such as the number of meta-atoms in a unit cell, the distance between the meta-atoms, the constituent materials and structural parameters of every meta-atom, and the structural symmetry of every meta-atom and the whole unit cell. A lot of related works have been published in the past several years, which validates the great advantages of few-layer metasurfaces and polyatomic metasurfaces for high-efficient, multi-band and broadband wave control [20,23–26]. Meanwhile, novel EM functionalities that cannot be realized or are difficult to be achieved in single-layer monoatomic metasurfaces, such as the giant three-dimensional chirality, the asymmetric transmission of linear-polarized waves and the full-space manipulation of EM waves, have also been well demonstrated in few-layer metasurfaces and polyatomic metasurfaces [27–34].

In general, there are two main strategies to design few-layer metasurfaces and polyatomic metasurfaces (Fig. 1): the direct superposition strategy and the collective interference strategy. For few-layer metasurfaces and polyatomic metasurfaces designed based on the direct superposition strategy, the resonances of meta-atoms in the unit cell can be independently designed to be at different operation wavelengths or for orthogonal polarization states. Thus, the couplings between the meta-atoms in a unit cell is negligible. On the contrary, for few-layer metasurfaces and polyatomic metasurfaces designed based on the collective interference strategy, the neighbor interactions between the meta-atoms in a unit cell play a decisive role in the EM responses of metasurfaces. The above-mentioned two design strategies have been widely utilized in the design of few-layer metasurfaces and polyatomic metasurfaces. The direct superposition strategy is usually used for the realization of frequency- and polarization-selective multifunction integration, while the collective interference strategy is widely used to enhance the light-matter interactions and realize novel EM responses with high efficiency and broad operational bandwidth.

Here, we review the recent advances of few-layer metasurfaces and polyatomic metasurfaces from the viewpoint of their design strategies. In Sections 2 and 3, we present some representative works of few-layer metasurfaces and polyatomic metasurfaces respectively and discuss their advantages for EM wave manipulation. The applicability of the two design strategies is also validated in these two sections. In the last section, we offer an outlook on future possible development trends and potential applications in these fast-developing research areas.

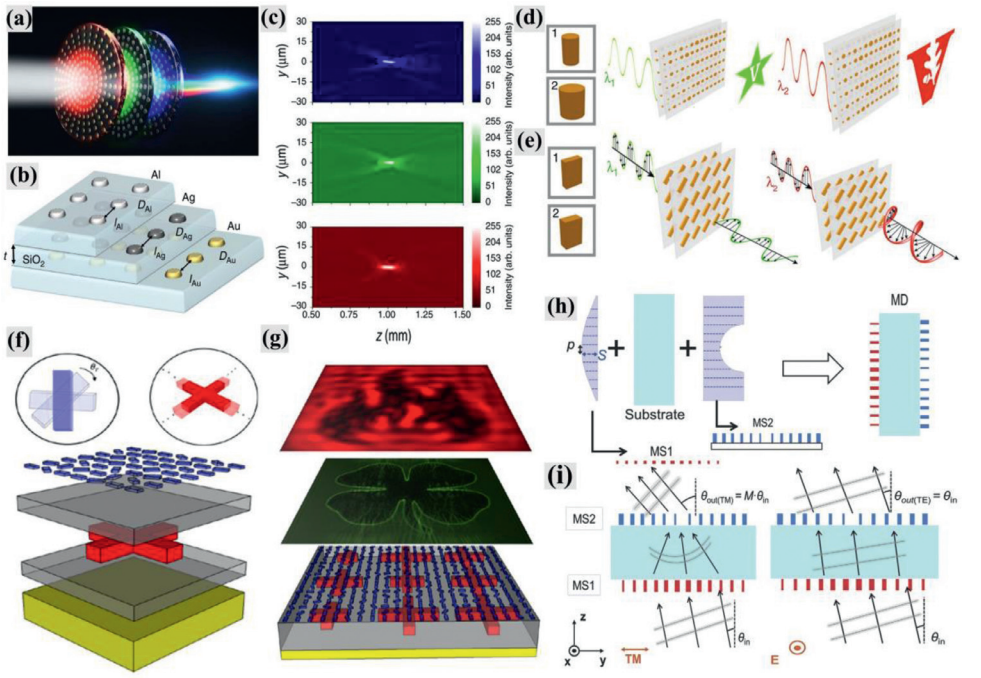

Fig. 2. Few-layer metasurfaces designed based on the direct superposition strategy. (a) Schematic of a multispectral achromatic lens based on a tri-layer composite plasmonic design. (b) Schematic of the tri-layer composite structure, each layer consists of different materials (gold, silver and aluminum) and works as a narrow-band Fresnel lens at a certain wavelength with a given focal point. (c) Experimentally measured intensity profiles for the achromatic lens under different illuminated wavelengths: 450 nm, 550 nm and 650 nm (from top to bottom). (d) Illustration of a dual-wavelength holography based on a bilayer metasurface. (e) Illustration of a dual-wavelength waveplate based on a bilayer metasurface, which acts as a half-wave plate at λ_1 and a quarter-wave plate at λ_2 respectively. (f) Schematic of the bilayer metasurface for multispectral holography. The two insets show the unit cells in the two layers, which are composed of meta-atoms with different shapes and materials. (g) Numerically calculated dual-wavelength out-plane holography image in the thermal infrared (37 THz) and visible (531 THz) spectra range respectively. (h) Illustration of the design principle of the all-dielectric two-layer multifunctional metasurface. (i) Schematic of the polarization-selective multifunctional beam control based on the bilayer metasurface. (a)–(c) Reproduced with permission from ref. [36], under the terms of the CC-BY Creative Commons Attribution 4.0 International License, copyright 2017, The Authors, published by Springer Nature. (d), (e) Reproduced with permission from ref. [37], copyright 2019, Spring Nature. (f), (g) Reproduced with permission from ref. [39], copyright 2018, American Chemical Society. (h), (i) Reproduced with permission from ref. [41], copyright 2020, Wiley-VCH (For interpretation of the references to color in this figure, the reader is referred to the web version of this article.).

2. Manipulating EM waves with few-layer metasurfaces

Thanks to the diverse interlayer couplings mechanisms, few-layer metasurfaces composed of more than one functional layer emerged as a versatile platform for the realization of EM functionalities with high efficiency and broad operation bandwidth. Moreover, the structural symmetries of few-layer metasurfaces can be arbitrarily designed. Novel EM functionalities that cannot be implemented by the planar metasurfaces can be realized in few-layer metasurfaces. Meanwhile, for few-layer metasurfaces in which the interlayer interactions are negligible, different EM functionalities can be independently engineered in each layer, resulting in the integration of multiple functionalities. In this section, we discuss the recent progress of few-layer metasurfaces for EM wave manipulation from the viewpoint of their design strategies.

2.1. Few-layer metasurfaces designed based on the direct superposition strategy

In few-layer metasurfaces, the interactions between the layers can be neglected when the resonances of the meta-atoms in each layer are designed to be at different operation wavelengths or for two orthogonal polarization states, or when the distances between the layers are far enough. By individually designing the particular EM functionality of each layer in a few-layer metasurface, wavelength-selective and multifunctional meta-devices with low cross-work and high performance can be accomplished [35–46]. For example, Avayu et al. achieved a triplet (red, green and blue) achromatic metalens by utilizing a tri-layer composite plasmonic metasurface, as shown in **Fig. 2**a,b [36]. In this design, the constituent material of meta-atoms in each layer is different and every layer can be viewed as a narrow-band binary Fresnel lens designed at a specific operation wavelength. Thus, this design can focus the incident light at three different wavelengths to the same focal position by adjusting the focus length of each layer independently. As shown in Fig. 2c, experimentally measured intensity profiles under different illuminated wavelengths of 450, 550 and 650 nm indicate the clear aberration correction.

Compared with planar monatomic achromatic metasurfaces in which the optical response of each meta-atom should be carefully designed in a broad bandwidth, few-layer metasurfaces provide a new pathway to realize achromatic applications. The direct superposition strategy utilized in the design of few-layer metasurfaces also provides an effective approach for the realization of wavelength-selective multifunction integration. As illustrated in Fig. 2d, a bilayer metasurface composed of two layers of amorphous silicon nanoposts can generate two different holography images at two different wavelengths (λ_1 = 1180 and λ_2 =1680 nm). Each layer of this bilayer metasurface were utilized to independently control the phase profiles of the transmission waves at a certain wavelength, resulting in the wavelength-selective optical holography [37]. By using the same design principle, a bilayer metasurface that acts as a half-wave plate at λ_1 = 1200 nm and a quarter-wave plate at λ_2 = 1600 nm was designed and demonstrated, as shown in Fig. 2e. Obviously, tightly spaced few-layer noninteracting dielectric metasurfaces show unprecedented application possibilities in multiwavelength metaoptics [38].

In the above-mentioned few-layer metasurfaces for wavelength-selective multifunction integration, the operation wavelengths are close to each other. Actually, the wavelength ratio of different operating channels can be freely modified. For example, Forouzmand et al. proposed a bilayer indium tin oxide (ITO)-dielectric composite structure which consists of the silicon nanorods in the top layer and the ITO cross-shaped nano-antennas in the bottom layer, as shown in Fig. 2f [39]. Owing to the diverse optical properties of the highly doped ITO in different frequency ranges, the meta-atoms in the two layers can be individually designed to realize different optical functionalities at two wavelengths that are far apart. Calculated results in Fig. 2g showcase that the proposed design can realize a dual-wavelength optical holography with operation wavelengths in the thermal infrared (37 THz) and visible (531 THz) spectral region respectively.

Few-layer metasurfaces designed based on the direct superposition strategy can not only be utilized to implement the combination of EM functionalities with different operation wavelengths, but also be good alternatives to combine different EM functionalities at a certain wavelength. For example, Basiri et al. proposed a bilayer chiral metasurfaces designed based on Jones matrix method to realize the spin-selective transmission of circular-polarized waves [40]. The unit cell of the designed bilayer metasurfaces is composed of an anisotropic nanostructure acting as a quarter waveplate, a linear polarizing nanograting, and a dielectric spacer layer between these components. Recently, Zhou et al. proposed a bilayer all-dielectric metasurface doublet for multifunctional beam control at telecommunication wavelengths, as shown in Fig. 2h,i [41]. The meta-atom in each layer is subwavelength hydrogenated amorphous silicon (a-Si:H) gratings that are corresponding to the predefined phase profiles. Analogous to the conventional doublet lens, the optical functionality of each layer in the proposed bilayer metasurface can be treated as a convex lens with a focal length f and a concave lens with a focal length of f/M respectively, as illustrated in Fig. 2h. Owing to the polarization-dependent phase profiles design, the proposed bilayer metasurface can travel the TE-polarized light straightly following the angle of incidence and deflect the TM-polarized light at three times the incident angle with the reduced beam width by half, as shown in Fig. 2i. Different from above-mentioned few-layer metasurfaces which are closely spaced in order to basically meet the design requirements of eliminating interlayer coupling, here two arrays of rectangular nano-resonators were manufactured on either side of a quartz substrate. In this way, multiple metasurfaces can be vertically integrated to form metasystems. Several miniature optical systems with high performance and low loss have been proposed, including an aberration-corrected planar camera, a metasurface retroreflector and a single-shot quantitative phase gradient microscopy [47–50].

Few-layer metasurfaces designed based on the direct superposition strategy show great advantages on EM multifunctional integration, which significantly improve the wave-control capabilities of metasurfaces.

2.2. *Few-layer metasurfaces designed based on the collective interference strategy*

In addition to designing each functional layer independently, few-layer metasurfaces with abundant interlayer interactions (such as near-field coupling effect, multiple wave interference effect and waveguide effect) provide an extra design freedom to enhance the interactions between EM waves and metasurfaces. For example, by utilizing the strong near-field coupling effect between the meta-atoms in the two layers, enhanced chiroptical responses can be realized in chiral bilayer metasurfaces [51–54].

Thanks to the existence of the rich interlayer interactions, few-layer metasurfaces that enable flexible manipulation of EM waves, largely boost the achievements of new functional metasurfaces for a variety of applications [55–63]. **Fig. 3**a shows a unit cell of a Huygens' bilayer metasurface which can realize a full-phase control of the transmitted wave at the microwave frequencies by varying the impedance of the reflectionless sheets in the two layers [55]. The unit cell of this Huygens' metasurface is composed of a pair of copper patterns on the top layer and a split-ring resonator on the bottom layer, which provide the required electric and magnetic polarization currents respectively. The simulated magnetic field distribution in Fig. 3b shows a clear anomalous refraction of EM waves for the proposed metasurface under y-polarization normal incidence, and Fig. 3c shows the experimentally measured and numerically simulated anomalous refraction efficiency. These results validate the high-efficiency and broadband performance of the proposed Huygens' bilayer metasurface. By utilizing the similar structural configurations, high-efficient wavefront control has further been implemented in the near-infrared and mid-infrared regions [64,65].

Not only the near-field coupling effect, but also the multiple wave interference effect can be utilized to enhance the couplings between the EM waves and the meta-atoms. As shown in Fig. 3d, Li et al. proposed a bilayer aluminum metasurface to realize a broadband and near-perfect linear polarizer by utilizing the multiple wave interference effect [56]. The experimentally measured transmittance spectra of the bilayer metasurface under linear-polarized illuminations with different polarized angles α and incident wavelengths show a good agreement with the theoretically calculated result based on the Malus' law, as shown in Fig. 3e. Compared with the single-layer metasurface composed of aluminum nanorods, the bilayer metasurface presents a broader operational bandwidth and a higher polarization-selective extinction ratio, as shown in Fig. 3f. Specifically, for few-layer metasurfaces that designed by utilizing the wave interference effect, the degree of misalignment between the layers always has a negligible effect on the optical response. This feature lower the high alignment requirement on the fabrication process, which enable the realization of the alignment-free high-efficient asymmetric transmission and bidirectional perfect absorption [66,67].

Different from the above-mentioned two interlayer interactions that are mainly utilized to improve the efficiency and operation bandwidth of few-layer metasurfaces, the waveguide effect in few-layer metasurfaces provide a direct way for the phase manipulation of EM waves. As shown in Fig. 3g, a bilayer plasmonic metasurface composed of a pair of nano-apertures was proposed to achieve simultaneous control of polarization and phase of the transmitted light [57]. For this design, the polarization state of the transmitted light can be controlled by adjusting the oriented angle of the nano-aperture since only linear-polarized incident light with polarization direction perpendicular to the major axis of nanoaperture is allowed to pass through. Meanwhile, the phase of the transmitted light is partly decided by the waveguide effect within the two layers, which can be designed by adjusting the alignment parameter S between the two layers. The phase of the transmitted waves then can be fully tuned by changing the length L of the nano-apertures and the lateral translation S. Fig. 3h shows sixty rectangular nanoaperture pairs with varied geometrical dimensions and orientations that can realize the simultaneous control of light polarization and phase. With the combinations of these nanoaperture pairs, a radially polarized beam under circularly polarized incident light were experimentally generated, as shown in Fig. 3i. Actually, since polarization and phase of the transmitted light can be fully manipulated, these nanoaperture pairs can be utilized to realize vector beams with arbitrary spatial distribution of phase and polarization [64]. A recent approach further validates that the waveguide effect in few-layer metasurfaces can be used to realize the bidirectional perfect absorption of light waves [68,69].

Normally, the unit cells in a few-layer metasurface are designed one by one to full fill the desired complex amplitude profile associated to a certain EM functionality. Different from this generic design concepts, Raeker et al. proposed a modified phase-retrieval algorithm to realize the independent design of the complex amplitude profile of two phase-discontinuous metasurfaces in a compound meta-optics layout [58]. As illustrated in Fig. 3j, the two metasurfaces separated a wavelength-scale distance was proposed to freely reshape the amplitude and phase profiles of an incident beam on demand. The modified phase-retrieval algorithm was used to produce the abrupt phase profiles of the two metasurfaces by taking two complex-valued electric field profiles (E_{inc} and E_{des}) as inputs. Then, the two metasurfaces can be realized by bianisotropic Huygens metasurfaces composed of a cascade of electric impedance sheets at microwave frequencies due to their reflectionless, passive and lossless characteristics [70]. Based on this design approach, the amplitude and phase profiles of the scattered field can be independently controlled. This approach provides a new perspective to the design of few-layer metasurfaces. Likewise, compound meta-optics components constructed by two lossless all-dielectric phase-only metasurfaces can realize the high-efficient independent amplitude and phase manipulation of light waves [71,72]. Note that, with the rapid development of artificial intelligence assisted nano-photonics designs, few-layer metasurfaces in-

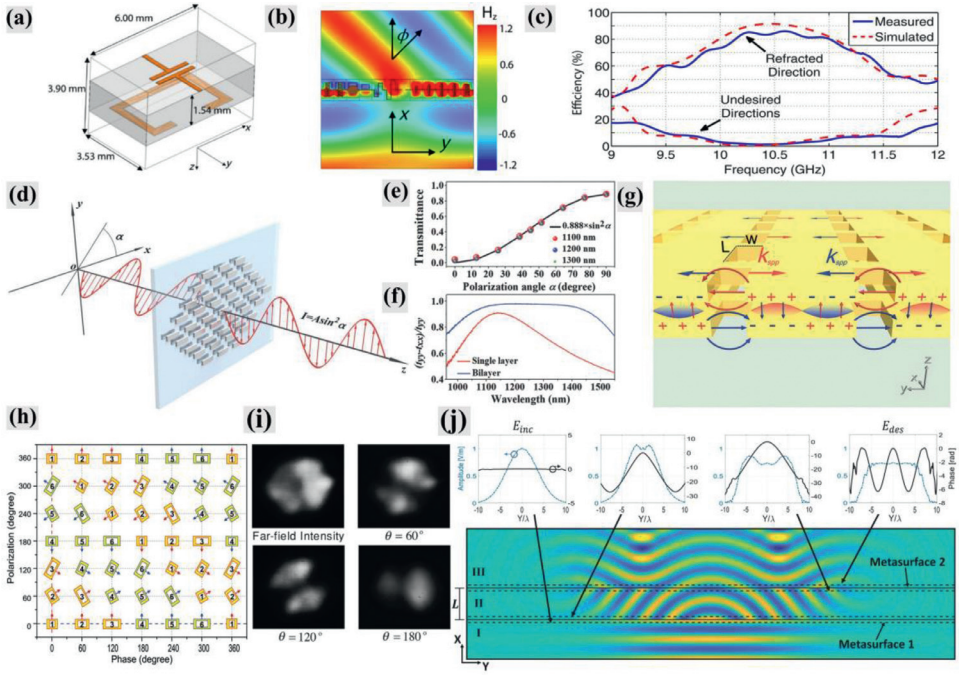

Fig. 3. Few-layer metasurfaces designed based on the collective interference strategy. (a) Unit cell of the Huygens' dual-layer metasurface for achieving broadband anomalous refraction in the microwave region. (b) Simulated magnetic field (H_z) distribution of the Huygens' metasurface for *y*-polarization normal incidence. (c) Experimentally measured and numerically simulated anomalous refraction efficiency of the Huygens' metasurface. (d) Illustration of the polarization-selective transmission via the bilayer aluminum metasurface. (e) Experimentally measured transmittance as a function of polarization angle α under linear-polarized illumination at 1100 nm, 1200 nm and 1300 nm. The solid line represents the theoretically calculated result based on the Malus' law. (f) Comparison of the transmission ratio between the single layer metasurface composed of nanorods and the bilayer metasurface. (g) Schematic of the bilayer plasmonic metasurface composed of aligned nanoaperture pairs, in which the waveguide mode is excited. (h) Schematic illustration of the nanoaperture pairs with various dimensions and directions that can realize the simultaneous control of light polarization and phase distributions. (i) Experiment results of a generated vector beam for bilayer metasurfaces composed of units 1–6 in (h). The measured far-field intensity profiles representing a radially polarized beam without and with a polarizer (oriented at angle θ) intercepted before the CCD camera. (j) Schematic illustration of the reflectionless bilayer metasurface for arbitrarily reshaping the amplitude and phase profiles of an incident beam. The insets show the amplitude and phase profiles of the electric field before and after each metasurface (E_{inc} and E_{des}). Because the absorption, reflection and polarization losses are eliminated, local power flux through the boundaries of each metasurface remain conversed. (a)–(c) Reproduced with permission from ref. [55], copyright 2013, American Physical Society. (d)–(f) Reproduced with permission from ref. [56], copyright 2019, Wiley-VCH. (g)–(i) Reproduced with permission from ref. [57], copyright 2015, Wiley-VCH. (j) Reproduced with permission from ref. [58], copyright 2019, American Physical Society.

verse design based on deep-learning methods and various optimization algorithms provide another effective approach to implement complex and high-performance wave control [73–76].

Overall, the interlayer interaction within few-layer metasurfaces is a useful design freedom for high-performance and multidimensional EM wave manipulation.

3. Manipulating EM waves with polyatomic metasurfaces

Compared to few-layer metasurfaces in which the multiple meta-atoms in a unit cell are introduced in the direction perpendicular to the surface, planar polyatomic layout provides another effective approach to extend the design freedom of metasurfaces. In polyatomic metasurfaces, the meta-atoms in a unit cell are introduced in the direction parallel to the surface. The advantages of polyatomic metasurfaces for EM wave manipulation can be divided into two parts: on the one hand, by judiciously interleaving the meta-atoms in which the resonances are independently designed to be at different wavelengths or for two orthogonal polarization states, polyatomic metasurfaces are ideal candidates to integrate diversified functionalities into single devices with subwavelength thickness and high efficiency. On the other hand, the couplings between the meta-atoms in a unit cell can significantly enhance the light-matter interactions, and the interference effect in the polyatomic metasurfaces is a powerful tool to realize polarization-selective transmission. In this section, typical researches in the past decade for EM waves manipulation with polyatomic metasurfaces are discussed from the viewpoint of their design strategies.

3.1. Polyatomic metasurfaces designed based on the direct superposition strategy

Polyatomic metasurfaces designed based on the direct superposition strategy, in which the interactions between the meta-atoms in a unit cell have negligible effect on their EM responses, have been widely used to realize versatile EM wave manipulation and multifunction integration. For instance, a diatomic metasurface composed of two meta-atoms with opposite chiral optical responses were proposed to realize the spin-selective optical hologram [77]. An polyatomic metasurface composed of four nanodisks in one unit cell were utilized to realize color mixing, and 260 mixed structural colors were produced by the combination of eight basic nanodisks with different diameters [78].

Polyatomic metasurfaces was previously used for the implementation of multi-band and broadband wave absorption. Shen et al. proposed a microwave triple-band absorber composed of three nested closed-ring resonators in a unit cell, and every resonator is associated with an certain absorption peak [79]. Further, a broadband near perfect absorber in the near infrared regime was numerically and experimentally demonstrated based on a polyatomic metasurface [80]. As shown in **Fig. 4**a, the unit cell of the proposed absorber can be regarded as the combination of two kinds of meta-atoms: the outer layer cut wire and the inner layer cut wire (as shown in the insets of Fig. 4b). According to the absorption spectra and current distributions in Fig. 4b and c, these two kinds of meta-atoms can be periodically arranged respectively to form two optical absorbers whose operation wavelengths are adjacent. When combing the two kinds of meta-atoms into a unit cell, the resonant peaks are merged in the absorption spectrum as a result of the hybridization of the electric dipoles, producing the broadband near perfect absorber.

Nowadays, polyatomic metasurfaces designed based on the direct superposition strategy have emerged as a powerful platform for multicolor meta-hologram. To realize the multicolor meta-hologram utilizing polyatomic metasurfaces, firstly, meta-atoms that can achieve the phase manipulation of EM waves at different operation wavelengths were designed. Then, meta-holograms with high resolution and low crosstalk were demonstrated by arranging these meta-atoms in a unit cell. For example, Wang et al. reported a polyatomic dielectric metasurface composed of four nanorods in one unit cell to realize the simultaneous and

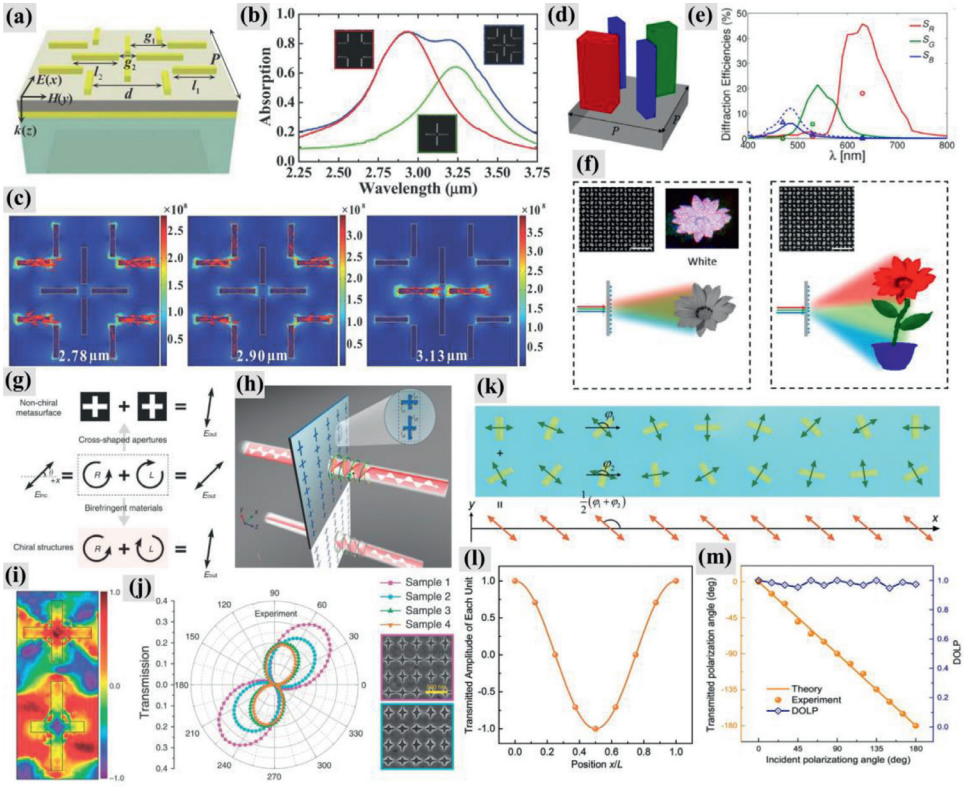

Fig. 4. Polyatomic metasurfaces designed based on the direct superposition strategy. (a) Schematic of a unit cell of the broadband near perfect absorber. (b) Experimental absorption spectra of the outer structure (red line), the inner structure (green line), and the whole structure (blue line). Inset: SEM images of the corresponding structures. (c) The surface current distribution and the electric field modulus on the surface of the metasurface. (d) Schematic of the unit cell of the polyatomic metasurface, which consists of four Si nanoblocks. (e) Simulated spectra of the diffraction efficiency of the red, green, and blue nanoblocks respectively. (f) Schematic of the multiwavelength achromatic and highly dispersive meta-holograms based on polyatomic metasurfaces. Inset: SEM images of the fabricated metasurfaces and the experimental result of the achromatic color hologram. (g) Comparison between the theories of controllable optical activity. (h) Schematic of the optical activity in the non-chiral diatomic metasurface. (i) Normalized Stokes parameters S_3 in the near-field (5 nm from the exit surface of a unit cell composed of two cross-shaped nanostructures). (j) Experimental results of the transmittances and optical rotations of the output light for four diatomic metasurfaces with different structural parameters. Inset: the SEM images of sample 1 and sample 2. (k) Schematic of a supercell of the designed half-wave plate. The unit cell in each column is composed of two anisotropic metal antennas with different orientation angles φ_1 and φ_2, the orange arrows show the constant optical axis in the direction $(\varphi_1+\varphi_2)/2$. (l) Transmission amplitude of the unit cell in every column as a function of the position in the row. (m) Theoretical (orange line) and measured (orange symbols) polarization angle of the transmitted light for different incident polarization angles. The degrees of linear polarization are given by the blue symbols at the corresponding incident polarization angles. (a)–(c) Reproduced with permission from ref. [80], copyright 2011, AIP Publishing. (d)–(f) Reproduced with permission from ref. [81], copyright 2016, American Chemical Society. (g)–(j) Reproduced with permission [87], copyright 2016, Nature Publishing Group. (k)–(m) Reproduced with permission [88], copyright 2017, American Chemical Society (For interpretation of the references to color in this figure legend, the reader is referred to the web version of this article.).

independent phase manipulation of the three-color light, as shown in Fig. 4d [81]. The blue, green and red nanorods serve as half-wave plates at three adjacent wavebands (the blue, green and red light). Based on the concept of geometric phase, these nanorods can realize the phase manipulation of the trichromatic circular-polarized light respectively by setting their in-plane orientations. Two blue nanorods for the phase manipulation of blue light are utilized in a unit cell since the diffraction efficiency of the blue nanorods are lower than the green and the red ones, as shown in Fig. 4e. The experiment results in Fig. 4f validate the capabilities of the proposed polyatomic dielectric metasurface for the realization of multiwavelength achromatic color hologram and highly dispersive color hologram. With a similar design configuration, polarization-controlled color-tunable optical holograms was further demonstrated, in which the color of not only the entire holographic image but also its definite part can be modulated by changing the polarization of the incident light [82]. By utilizing the incident angle as a new design freedom, the holographic images generated by polyatomic metasurfaces can be further modulated by polarization, wavelength and the incident angle of optical waves at the same time, which significantly expand the flexibility of metasurface for multichannel optical hologram [83]. Besides the multicolor meta-hologram, polyatomic metasurfaces designed based on the direct superposition strategy are also good alternatives to implement polarization-controlled color images [84,85].

With the combination of two meta-atoms in a unit cell, polyatomic metasurfaces show great advantages to individually manipulate EM waves with orthogonal polarization states. For example, Deng et al. realized polarization-multiplexed metagrating holograms by perpendicularly interleaving the aligned nanorod pair [86]. As another example, Yu et al. proposed a non-chiral diatomic metasurface to realize controllable optical activity, as shown in Fig. 4g to j [87]. The unit cell of the proposed diatomic metasurface consists of two cross-shaped aluminum nanostructures with different structural parameters. The two nanostructures can convert the linear-polarized incident light into left-handed and right-handed circularly polarized transmitted light respectively in the near field (Fig. 4i), and the phase difference between the two different polarizations of transmitted light can be modulated by varying the structural parameters of the cross-shaped nanostructures. As shown in Fig. 4g, similar to natural chiral materials, optical activity can be observed in the proposed non-chiral diatomic metasurface. By adjusting the phase difference between the left-handed and right-handed circularly polarized transmitted light in the near field, the linear-polarized transmitted light whose polarization direction is different from the incident one can be generated in the far field. The experimental results in Fig. 4j validate a continuously controllable optical activity from 3 degrees to 42 degrees.

Recent approaches further prove that polyatomic metasurfaces can be utilized to realize the wavefront and polarization manipulation of EM waves simultaneously [88–93]. Liu et al. demonstrated a new strategy for realizing broadband half-wave plate with polyatomic metasurface, as shown in 4k to 4m [88]. The structural configuration of the proposed polyatomic metasurface is shown in Fig. 4k. Two nano-antennas with different orientation angles φ_1 and φ_2 in each column form a half-wave plate, and the half-wave plate in each column has the same optical axis. Therefore, for linear-polarized incident light with the polarization angle of φ, the linear-polarized transmitted light with the polarization angle of $\varphi_1 + \varphi_2 - \varphi$ will be generated. As shown in Fig. 4m, when the optical axis of the half-wave plate is fixed, experimentally measured and theoretically predicted polarization angle of the transmitted light

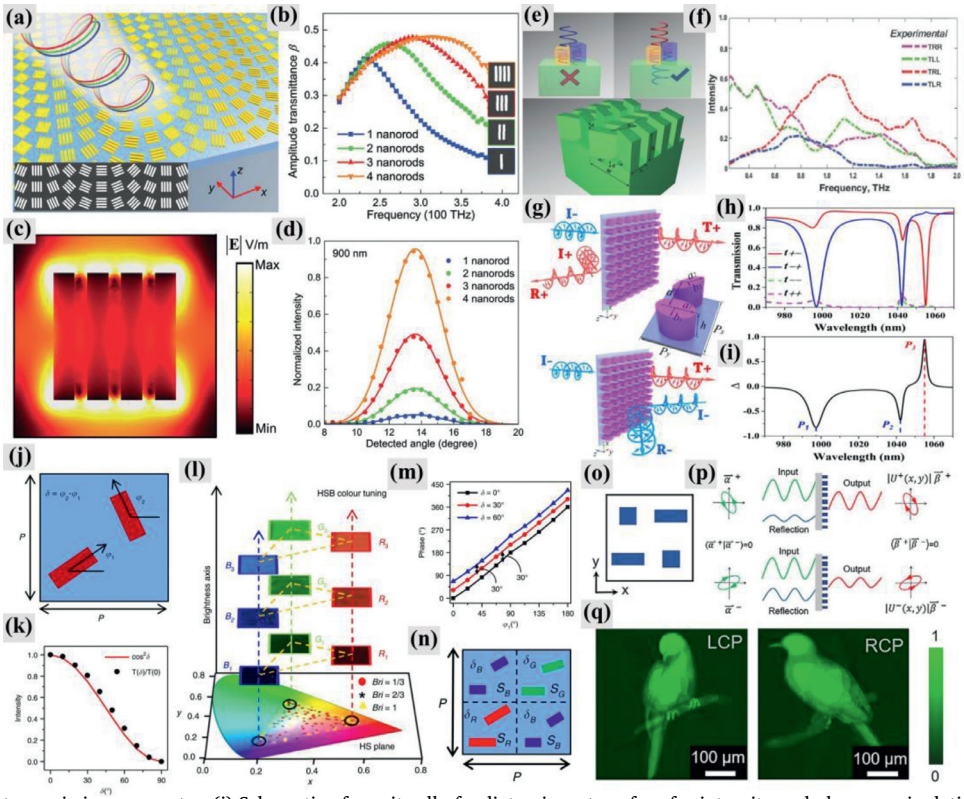

Fig. 5. Polyatomic metasurfaces designed based on the collective interference strategy. (a) Schematic of the multi-nanorod metasurface for realizing abnormal refraction. Inset: the SEM images of the metasurface. (b) Calculated amplitude transmittance of the anomalous refracted light for metasurfaces with different numbers of nanorods. Inset: the SEM images of the unit cell containing different numbers of nanorods. (c) Electric field distribution in a resonant unit cell of the metasurface composed of four nanorods at the resonant frequency. (d) The normalized intensity of refraction light as a function of the observation angle at wavelength 900 nm. (e) Schematic illustrating the spin-selective transmission in a diatomic metasurface. Top: Schematic of the functionality for right-handed circular-polarized (blue) and left-handed circular-polarized (red) incident light. Bottom: Schematic of structural configuration of the designed diatomic metasurface. (f) Normalized experimental values of co-polarized and cross-polarized transmission intensity for the diatomic metasurface. (g) Schematic of the spin-selective transmission and asymmetric transmission in a diatomic dielectric metasurface. (h) Simulated results of the module square of the four transmission coefficients of the diatomic metasurface and (i) the calculated results of the asymmetric transmission parameter. (j) Schematic of a unit cell of a diatomic metasurface for intensity and phase manipulation of the transmitted light, the unit cell consists of two identical c-silicon nanoblocks with rotation angles of φ_1 and φ_2 relative to the x-axis. (k) Simulated results of the intensity variation of the transmitted light as a function of angle δ in the diatomic metasurface and (l) schematic diagram of realizing HSB color tuning based on the intensity tuning. (m) Simulated results of the phase variation of the transmitted light as a function of angle φ_1 in the diatomic metasurface. (n) Schematic of the RGB super unit cell composed of four double-nanoblock subunits. (o) Schematic of a polyatomic metasurface composed of four dielectric nanoblocks and (p) the corresponding conceptual schematic diagram for the realization of independent amplitude control of arbitrary orthogonal states of polarization. (q) Experimentally captured optical images of a designed metasurface nanoprinting illuminated with LCP and RCP light. (a)–(d) Reproduced with permission from ref. [97], copyright 2015, Wiley-VCH. (e), (f) Reproduced with permission from ref. [100], copyright 2016, John Wiley and Sons. (g)–(i) Reproduced with permission from ref. [102], copyright 2019, OSA Publishing. (j)-(n) Reproduced with permission from ref. [107], copyright 2019, Springer Nature. (o)–(q) Reproduced with permission from ref. [108], copyright 2020, American Physical Society (For interpretation of the references to color in this figure legend, the reader is referred to the web version of this article.).

changes as a function of the polarization angle of the incident light, and the changing rule represents the optical responses of a half-wave plate. Meanwhile, under the condition that the optical axis of each column is unchanged, the wavefront (intensity distribution) of the transmitted cross-polarized waves can be manipulated by continuously varying the rotation angle of the meta-atoms along the row (Fig. 4l), which further ensures the degree of linear polarization of the transmitted light. Moreover, full-polarization generation and control have also been realized in polyatomic metasurfaces, which have been applied to realize the vectorial meta-hologram and the polarization-maintaining meta-hologram [89–91]. By judiciously designing positions and rotation angles of two identical meta-atoms, perfect vector vortex beams with arbitrary polarization, independent amplitude and phase distributions were also successfully generated [93].

We can see from the above-mentioned works that polyatomic metasurfaces designed based on the direct superposition strategy show endless possibilities for the implementation of multi-band and broadband EM wave manipulation, multicolor meta-hologram, color imaging, polarization manipulation of EM waves and polarization- and wavelength-selective multifunction integration.

3.2. Polyatomic metasurfaces designed based on the collective interference strategy

The couplings between the meta-atoms in a unit cell can significantly enhance the light-matter interactions, which is a powerful design freedom to improve the performance of meta-devices and achieve new EM functionalities [94–108]. Generally, the collective interference within polyatomic metasurfaces mainly affect the intensity of transmission and reflection waves. For example, Liu et al. proposed a polyatomic metasurface composed of four gold nanorods in one unit cell to realize abnormal refraction with efficiency close to the theoretical limitation, as shown in **Fig. 5**a to d [97]. With the increasing of the number of the nanorods in a unit cell, the amplitude of the cross-polarized transmission coefficient significantly increases (Fig. 5b), and the working waveband expands simultaneously. These can be attributed to the strong near-field couplings between the nanorods (Fig. 5c), which resulting in the strong enhancement of the radiation damping and hybridization. The result in Fig. 5d further validates that the efficiency of the abnormal refraction can be significantly improved by increasing the number of nanorods in the unit cell. Meanwhile, the near-field coupling effect in polyatomic metasurfaces also provide a good alternative for the realization of the quasi-bound states in the continuum [98,99].

Recently, polyatomic metasurfaces were widely used to realize polarization-selective transmission/reflection of EM waves by utilizing the collective interference between meta-atoms [100–106]. As shown in Fig. 5e to f, a diatomic metasurface was proposed to realize the spin-selective transmission of optical waves [100]. The proposed diatomic metasurface is composed of two dielectric nanoblocks, and one nanoblock is elevated with a certain thickness relative to the other to introduce the $\pi/2$ difference in propagating phase. The two nanoblocks, which form a $\pi/8$ angle with respect to the symmetry line, can be treated as two half-wave plates. Thus, the circular-polarized beam can be completely converted to the opposite polar-

ization state and a phase delay of $\pm\pi/2$ (the sign + and − corresponding to right-handed and left-handed circular-polarized incident waves) can be added, when light passing through these two nanoblocks. Thus, for left-handed circular-polarized incident waves, the phase difference between the waves passing through the two nanoblocks equals to zero, corresponding to constructive interference and high transmittance. On the contrary, for right-handed circular-polarized incident waves, the phase difference between the waves passing through the two nanoblocks equals to π, corresponding to destructive interference and low transmittance. Based on the same design principle, asymmetric transmission of circular-polarized waves and three spin-selective optical functionalities (light beam deflection, vortex beam generation and optical hologram) were achieved based on a polyatomic metasurface [101].

Apart from utilizing the phase difference between the meta-atoms, the excitation of overlapping multipolar resonances in the polyatomic metasurface can also be used to realize the spin-selective transmission. Ma et al. demonstrated spin-selective transmission and asymmetric transmission of circular-polarized waves in a diatomic dielectric metasurface by modulating the excitation and overlapping of the multipole resonances, as illustrated in Fig. 5g [102]. Giant spin-selective asymmetric transmission with efficiencies equal to −0.83, −0.68, and 0.94 can be observed at 997 nm, 1042 nm, 1055 nm, respectively, as shown in Fig. 5h and i. Compared to previous works based on planar metallic metasurface, the efficiency of asymmetric transmission in the proposed diatomic metasurface is significantly improved. A recent approach further validates that polarization-selective transmission of arbitrary orthogonal polarized light with nearly 100% theoretical efficiency and over 90% experimental efficiency can be realized by using diatomic metasurfaces designed based on the collective interference strategy [103].

Moreover, with the combination of the collective interference strategy and the direct superposition strategy, polyatomic metasurfaces are also good alternatives for the realization of light intensity manipulation at multiple wavelengths. Bao et al. proposed a diatomic metasurface to realize continuous intensity tuning of the three primary colors red, green and blue, so brightness tuning of colour has been well addressed [107]. As shown in Fig. 5j, the unit cell of the proposed metasurface consists of two silicon nanoblocks with the same structural configuration but an orientation angle difference of δ. Owing to the collective interference of light between the two nanoblocks, the intensity of the transmitted waves is proportional to $\cos^2\delta$. Thus, the intensity control of the individual colors can be achieved by altering the rotation angle difference δ, leading to the extrusion of the color gamut from the two-dimensional CIE space to a complete three-dimensional HSB space, as shown in Fig. 5k and l. Besides the intensity manipulation, the phase of the transmitted waves can also be controlled by changing the rotation angle φ_1 while keeping the rotation angle difference δ unchanged, as illustrated in Fig. 5m. By further utilizing the direct superposition strategy (Fig. 5n), the integration of HSB color printing and full-colour hologram can be well implemented.

Step further, Fan et al. demonstrated that arbitrary amplitude distributions can be imparted on two orthogonal polarization states by utilizing the collective interference of light in polyatomic dielectric metasurfaces, as illustrated in Fig. 5o to p [108]. As a typical application example, the lifelike bird images of a polyatomic metasurface nanoprinting are presented under two orthogonal circular polarization waves (Fig. 5q). Recent advances further validate that the collective interference of light in polyatomic dielectric metasurfaces can be utilized to realize the simultaneous and independent control of phase and amplitude for orthogonal polarization states [109,110].

The above-mentioned works prove the unprecedented controllability of polyatomic metasurfaces on the intensity manipulation of EM waves. Meanwhile, the couplings between the meta-atoms in the unit cell of polyatomic metasurfaces provide an efficient method to improve the performance of metasurfaces for EM wave manipulation.

4. Conclusions and outlook

Few-layer metasurfaces and polyatomic metasurfaces have more degrees of design freedom when compared with the single-layer monatomic ones, thus greatly improve the capacity, flexibility and controllability of metasurfaces for EM wave manipulation and produce new functional applications that were previously impossible to implement. We summarized the recent developments of few-layer metasurfaces and polyatomic designs from the viewpoint of their design strategy. These advances show the diversified wave-manipulation capabilities of few-layer metasurfaces and polyatomic metasurfaces, and exhibit a plethora of novel applications. Here, we present several promising research directions in these rapidly developing fields that may be foreseeable in the future.

By constructing few-layer metasurfaces in combination with polyatomic designs, the design freedoms of metasurfaces can be further expanded, which is quite benefit for the implementation of arbitrary manipulation of EM waves. Since their structural symmetries can be arbitrarily designed, few-layer polyatomic metasurfaces have been used to realize the devisable and high-efficiency three-dimensional optical chirality [111,112]. By cascading a pair of tightly spaced single-layer diatomic metasurface, chiral quasi-bound states in the continuum showing full circular dichroism at the resonance wavelength have been theoretically proposed [113]. Meanwhile, full-space and asymmetric control of EM waves has been designed and experimentally realized in few-layer polyatomic metasurfaces [114,115]. Predictable, few-layer polyatomic metasurfaces are playing an increasingly important role for EM wave manipulation.

Compared with the passive metasurfaces, active metasurfaces whose EM responses can be dynamically tuned in both spatial domain and time domain, result in a number of emerging new physics and technologies [116,117]. Correspondingly, active few-layer metasurfaces and polyatomic metasurfaces are good candidates to realize the dynamic control of high-performance and new functional EM applications. For instance, dynamic holograms for advanced optical information encryption have been realized based on polyatomic metasurfaces [118]. Recently, an electronically tunable polarization rotator also has been demonstrated based on few-layer metasurfaces [119]. The tunable few-layer and polyatomic metasurfaces provide a viable platform to create novel multifunctional and reconfigurable meta-devices.

Recent advances in nonlinear metasurface reveal the extensive application prospect of collective interference effect in the field of nonlinear optical filed manipulation. By utilizing nonlinear polyatomic metasurface designs, multidimensional optical information encoding has been achieved [120,121], which provides an effective pathway to realize nonlinear multifunctional applications.

Nowadays, few-layer metasurfaces have been widely utilized to realize the direct superposition of different functionalities, which is difficult to be implemented in the planar polyatomic designs. In a recent approach, a diatomic metasurface were proposed to realize the full-Stokes polarization perfect absorbers [122]. The unit cell of the proposed diatomic metasurface consists of two dissimilar meta-atoms that can control the perfect absorption and polarization of the outputting light respectively. This work represents a new design strategy, which can stimulate new functional applications based on polyatomic metasurfaces and their few-layer counterparts.

Besides these promising research directions, the further investigation and application of few-layer and polyatomic metasurfaces also face some critical challenges. For example, since the unit cell of a polyatomic metasurface consists of several meta-atoms, the period of the unit cell may be larger than the operation wavelength, resulting in the generation of additional diffraction orders and the reduction of efficiency. The non-negligible background noise from the co-polarized component in the polyatomic metasurfaces based on collective interference also lowers the performance of polyatomic metasurfaces, which can be eliminated by involving extra polarization detection condition during the

experimental measurement at the present stage. For few-layer metasurfaces with interlayer near-field interaction, the misalignment between the layers will significantly affect their optical responses, leading to a high requirement on the fabrication technology. Since few-layer and polyatomic metasurfaces have multiple degrees of design freedom, their design and optimization are much more complex when compare with the planar monatomic ones. Moreover, for few-layer and polyatomic metasurfaces designed based on the collective interference strategy, they usually have to be optimized as a whole, which inevitably causes increased design difficulty. Meanwhile, the effective theoretical tools that can reveal the underlying physics of these coupled system are still lacked. Overall, overcoming all these critical challenges will significantly put forward the development of few-layer and polyatomic metasurfaces. For instance, a rigorous theory derived from Maxwell's equations has recently been put forward to predict the line shapes of coupled plasmonic systems as required by manipulating the couplings between meta-atoms [123]. This work presents a formal theoretical framework for tailoring the optical responses of coupled photonic systems at will, and will contribute to the design of various new optical devices.

All in all, benefiting from the flexibly wave-manipulation capabilities of few-layer metasurfaces and polyatomic metasurfaces, a variety of high-performance and novel functional meta-devices have been proposed continuously. Therefore, it can expect that few-layer metasurfaces and polyatomic metasurfaces will trigger more advanced achievements in nano-photonics field.

Declaration of Competing Interest

The authors declare that they have no known competing financial interests or personal relationships that could have appeared to influence the work reported in this paper.

Acknowledgments

This work was supported by the National Key Research and Development Program of China (2017YFA0303800 and 2016YFA0301102), the National Natural Science Fund for Distinguished Young Scholar (11925403), the National Natural Science Foundation of China (11974193, 11904181,11904183, 91856101, and 11774186), Natural Science Foundation of Tianjin for Distinguished Young Scientists (18JCJQJC45700), and the China Postdoctoral Science Foundation (2018M640224 and 2021M690084).

References

[1] N.I. Zheludev, Obtaining optical properties on demand, Science 348 (2015) 973, doi:10.1126/science.aac4360.
[2] X. Luo, Principles of electromagnetic waves in metasurfaces, Sci. China Phys. Mech. Astron. 58 (2015) 594201, doi:10.1007/s11433-015-5688-1.
[3] D. Neshev, I. Aharonovich, Optical metasurfaces: new generation building blocks for multi-functional optics, Light Sci. Appl. 7 (2018) 58, doi:10.1038/s41377-018-0058-1.
[4] S. Sun, Q. He, J. Hao, S. Xiao, L. Zhou, Electromagnetic metasurfaces: physics and applications, Adv. Opt. Photonics 11 (2019) 380–479, doi:10.1364/aop.11.000380.
[5] K. Koshelev, Y. Kivshar, Dielectric resonant metaphotonics, Acs Photonics 8 (2020) 102–112, doi:10.1021/acsphotonics.0c01315.
[6] W. Liu, Z. Li, H. Cheng, S. Chen, Dielectric resonance-based optical metasurfaces: from fundamentals to applications, iScience 23 (2020) 101868, doi:10.1016/j.isci.2020.101868.
[7] W.T. Chen, F. Capasso, Will flat optics appear in everyday life anytime soon? Appl. Phys. Lett. 118 (2021) 100503, doi:10.1063/5.0039885.
[8] S. Chen, Z. Li, W. Liu, H. Cheng, J. Tian, From single-dimensional to multidimensional manipulation of optical waves with metasurfaces, Adv. Mater. 31 (2019) 1802458, doi:10.1002/adma.201802458.
[9] Y. Zhang, H. Liu, H. Cheng, J. Tian, S. Chen, Multidimensional manipulation of wave fields based on artificial microstructures, Opto Electron. Adv. 3 (2020) 200002, doi:10.29026/oea.2020.200002.
[10] A. Arbabi, Y. Horie, M. Bagheri, A. Faraon, Dielectric metasurfaces for complete control of phase and polarization with subwavelength spatial resolution and high transmission, Nat. Nanotechnol. 10 (2015) 937–943, doi:10.1038/nnano.2015.186.
[11] A.C. Overvig, S. Shrestha, S.C. Malek, M. Lu, A. Stein, C. Zheng, N. Yu, Dielectric metasurfaces for complete and independent control of the optical amplitude and phase, Light Sci. Appl. 8 (2019) 92, doi:10.1038/s41377-019-0201-7.
[12] C. Chen, S. Gao, X. Xiao, X. Ye, S. Wu, W. Song, H. Li, S. Zhu, T. Li, Highly efficient metasurface quarter-wave plate with wave front engineering, Adv. Photonics Res. 2 (2021) 2000154, doi:10.1002/adpr.202000154.
[13] Z. Li, W. Liu, Z. Li, C. Tang, H. Cheng, J. Li, X. Chen, S. Chen, J. Tian, Tripling the capacity of optical vortices by nonlinear metasurface, Laser Photonics Rev. 12 (2018) 1800164, doi:10.1002/lpor.201800164.
[14] S. Chen, W. Liu, Z. Li, H. Cheng, J. Tian, Metasurface-empowered optical multiplexing and multifunction, Adv. Mater. 32 (2020) 1805912, doi:10.1002/adma.201805912.
[15] Z. Li, W. Liu, G. Geng, Z. Li, J. Li, H. Cheng, S. Chen, J. Tian, Multiplexed nondiffracting nonlinear metasurfaces, Adv. Funct. Mater. 30 (2020) 1910744, doi:10.1002/adfm.201910744.
[16] S.M. Kamali, E. Arbabi, A. Arbabi, Y. Horie, M. Faraji-Dana, A Faraon, Angle-multiplexed metasurfaces: encoding independent wavefronts in a single metasurface under different illumination angles, Phys. Rev. X 7 (2017) 041056, doi:10.1103/PhysRevX.7.041056.
[17] W. Liu, Z. Li, Z. Li, H. Cheng, C. Tang, J. Li, S. Chen, J. Tian, Energy-tailorable spin-selective multifunctional metasurfaces with full fourier components, Adv. Mater. 31 (2019) 1901729, doi:10.1002/adma.201901729.
[18] A. Arbabi, A. Faraon, Fundamental limits of ultrathin metasurfaces, Sci. Rep. 7 (2017) 43722, doi:10.1038/srep43722.
[19] H.-H. Hsiao, C.H. Chu, D.P. Tsai, Fundamentals and applications of metasurfaces, Small Methods (2017) 1, doi:10.1002/smtd.201600064.
[20] S. Chen, Y. Zhang, Z. Li, H. Cheng, J. Tian, Empowered Layer effects and prominent properties in few-layer metasurfaces, Adv. Opt. Mater. 7 (2019) 1801477, doi:10.1002/adom.201801477.
[21] Y. Zhao, M.A. Belkin, A. Alu, Twisted optical metamaterials for planarized ultrathin broadband circular polarizers, Nat. Commun. 3 (2012) 870, doi:10.1038/ncomms1877.
[22] C. Pfeiffer, C. Zhang, V. Ray, L.J. Guo, A. Grbic, High performance bianisotropic metasurfaces: asymmetric transmission of light, Phys. Rev. Lett. 113 (2014) 023902, doi:10.1103/PhysRevLett.113.023902.
[23] H. Cheng, Z. Liu, S. Chen, J. Tian, Emergent functionality and controllability in few-layer metasurfaces, Adv. Mater. 27 (2015) 5410–5421, doi:10.1002/adma.201501506.
[24] H.T. Chen, A.J. Taylor, N. Yu, A review of metasurfaces: physics and applications, Rep. Prog. Phys. 79 (2016) 076401, doi:10.1088/0034-4885/79/7/076401.
[25] Z. Li, W. Liu, H. Cheng, S. Chen, Few-layer metasurfaces with arbitrary scattering properties, Sci. China Phys. Mech. Astron. 63 (2020) 284202, doi:10.1007/s11433-020-1583-3.
[26] G. Hu, M. Wang, Y. Mazor, C.-W. Qiu, A. Alù, Tailoring light with layered and moiré metasurfaces, Trends Chem. 3 (2021) 342–358, doi:10.1016/j.trechm.2021.02.004.
[27] Z. Li, H. Cheng, S. Chen, Few-layer metasurfaces with engineered structural symmetry, Sci. China Phys. Mech. Astron. 64 (2021) 264231, doi:10.1007/s11433-021-1687-x.
[28] S. Fasold, S. Linß, T. Kawde, M. Falkner, M. Decker, T. Pertsch, I. Staude, Disorder-enabled pure chirality in bilayer plasmonic metasurfaces, Acs Photonics 5 (2018) 1773–1778, doi:10.1021/acsphotonics.7b01460.
[29] C. Zhang, C. Pfeiffer, T. Jang, V. Ray, M. Junda, P. Uprety, N. Podraza, A. Grbic, L.J. Guo, Breaking Malus' law: Highly efficient, broadband, and angular robust asymmetric light transmitting metasurface, Laser Photonics Rev. 10 (2016) 791–798, doi:10.1002/lpor.201500328.
[30] T. Cai, G. Wang, S. Tang, H. Xu, J. Duan, H. Guo, F. Guan, S. Sun, Q. He, L. Zhou, High-efficiency and full-space manipulation of electromagnetic wave fronts with metasurfaces, Phys. Rev. Appl. 8 (2017) 034033, doi:10.1103/PhysRevApplied.8.034033.
[31] W.T. Chen, A.Y. Zhu, V. Sanjeev, M. Khorasaninejad, Z. Shi, E. Lee, F. Capasso, A broadband achromatic metalens for focusing and imaging in the visible, Nat. Nanotechnol. 13 (2018) 220–226, doi:10.1038/s41565-017-0034-6.
[32] J. Li, P. Yu, S. Zhang, N. Liu, A reusable metasurface template, Nano Lett. 20 (2020) 6845–6851, doi:10.1021/acs.nanolett.0c02876.
[33] M. Celebrano, X. Wu, M. Baselli, S. Grossmann, P. Biagioni, A. Locatelli, C. De Angelis, G. Cerullo, R. Osellame, B. Hecht, L. Duo, F. Ciccacci, M. Finazzi, Mode matching in multiresonant plasmonic nanoantennas for enhanced second harmonic generation, Nat. Nanotechnol. 10 (2015) 412–417, doi:10.1038/nnano.2015.69.
[34] Y. Yang, W. Wang, A. Boulesbaa, II Kravchenko, D.P. Briggs, A. Puretzky, D. Geohegan, J Valentine, Nonlinear fano-resonant dielectric metasurfaces, Nano Lett. 15 (2015) 7388–7393, doi:10.1021/acs.nanolett.5b02802.
[35] J. Ding, N. Xu, H. Ren, Y. Lin, W. Zhang, H. Zhang, Dual-wavelength terahertz metasurfaces with independent phase and amplitude control at each wavelength, Sci. Rep. 6 (2016) 34020, doi:10.1038/srep34020.
[36] O. Avayu, E. Almeida, Y. Prior, T. Ellenbogen, Composite functional metasurfaces for multispectral achromatic optics, Nat. Commun. 8 (2017) 14992, doi:10.1038/ncomms14992.
[37] Y. Zhou, II Kravchenko, H. Wang, H. Zheng, G. Gu, J Valentine, Multifunctional metaoptics based on bilayer metasurfaces, Light Sci. Appl. 8 (2019) 80, doi:10.1038/s41377-019-0193-3.
[38] Y. Zhou, II Kravchenko, H. Wang, J.R. Nolen, G. Gu, J Valentine, Multilayer noninteracting dielectric metasurfaces for multiwavelength metaoptics, Nano Lett. 18 (2018) 7529–7537, doi:10.1021/acs.nanolett.8b03017.

[39] A. Forouzmand, H. Mosallaei, Composite multilayer shared-aperture nanostructures: a functional multispectral control, Acs Photonics 5 (2018) 1427–1439, doi:10.1021/acsphotonics.7b01441.
[40] A. Basiri, X. Chen, J. Bai, P. Amrollahi, J. Carpenter, Z. Holman, C. Wang, Y. Yao, Nature-inspired chiral metasurfaces for circular polarization detection and full-Stokes polarimetric measurements, Light Sci. Appl. 8 (2019) 78, doi:10.1038/s41377-019-0184-4.
[41] C. Zhou, W.B. Lee, C.S. Park, S. Gao, D.Y. Choi, S.S. Lee, Multifunctional beam manipulation at telecommunication wavelengths enabled by an all-dielectric metasurface doublet, Adv. Opt. Mater. 8 (2020) 2000645, doi:10.1002/adom.202000645.
[42] H.X. Xu, G. Hu, M. Jiang, S. Tang, Y. Wang, C. Wang, Y. Huang, X. Ling, H. Liu, J. Zhou, Wavevector and frequency multiplexing performed by a spin-decoupled multichannel metasurface, Adv. Mater. Technol. 5 (2020) 1900710, doi:10.1002/admt.201900710.
[43] B. Groever, W.T. Chen, F. Capasso, Meta-lens doublet in the visible region, Nano Lett. 17 (2017) 4902–4907, doi:10.1021/acs.nanolett.7b01888.
[44] B. Yao, X. Zang, Z. Li, L. Chen, J. Xie, Y. Zhu, S. Zhuang, Dual-layered metasurfaces for asymmetric focusing, Photonics Res. 8 (2020) 830–843, doi:10.1364/PRJ.387672.
[45] Y. Hu, X. Luo, Y. Chen, Q. Liu, X. Li, Y. Wang, N. Liu, H. Duan, 3D-integrated metasurfaces for full-colour holography, Light Sci. Appl. 8 (2019) 86, doi:10.1038/s41377-019-0198-y.
[46] P. Georgi, Q. Wei, B. Sain, C. Schlickriede, Y. Wang, L. Huang, T. Zentgraf, Optical secret sharing with cascaded metasurface holography, Sci. Adv. 7 (2021) eabf9718, doi:10.1126/sciadv.abf9718.
[47] A. Arbabi, E. Arbabi, S.M. Kamali, Y. Horie, S. Han, A. Faraon, Miniature optical planar camera based on a wide-angle metasurface doublet corrected for monochromatic aberrations, Nat. Commun. 7 (2016) 13682, doi:10.1038/ncomms13682.
[48] A. Arbabi, E. Arbabi, Y. Horie, S.M. Kamali, A. Faraon, Planar metasurface retroreflector, Nat. Photonics 11 (2017) 415–420, doi:10.1038/nphoton.2017.96.
[49] H. Kwon, E. Arbabi, S.M. Kamali, M. Faraji-Dana, A. Faraon, Single-shot quantitative phase gradient microscopy using a system of multifunctional metasurfaces, Nat. Photonics 14 (2019) 109–114, doi:10.1038/s41566-019-0536-x.
[50] Y. Zhou, H. Zheng, I.I. Kravchenko, J. Valentine, Flat optics for image differentiation, Nat. Photonics 14 (2020) 316–323, doi:10.1038/s41566-020-0591-3.
[51] N. Liu, H. Liu, S. Zhu, H. Giessen, Stereometamaterials, Nat. Photonics 3 (2009) 157–162, doi:10.1038/nphoton.2009.4.
[52] X. Yin, M. Schaferling, B. Metzger, H. Giessen, Interpreting chiral nanophotonic spectra: the plasmonic Born-Kuhn model, Nano Lett. 13 (2013) 6238–6243, doi:10.1021/nl403705k.
[53] X. Yin, M. Schaferling, A.K. Michel, A. Tittl, M. Wuttig, T. Taubner, H. Giessen, Active chiral plasmonics, Nano Lett. 15 (2015) 4255–4260, doi:10.1021/nl5042325.
[54] V.E. Ferry, M. Hentschel, A.P. Alivisatos, Circular dichroism in off-resonantly coupled plasmonic nanosystems, Nano Lett. 15 (2015) 8336–8341, doi:10.1021/acs.nanolett.5b03970.
[55] C. Pfeiffer, A. Grbic, Metamaterial Huygens' surfaces: tailoring wave fronts with reflectionless sheets, Phys. Rev. Lett. 110 (2013) 197401, doi:10.1103/PhysRevLett.110.197401.
[56] Z. Li, W. Liu, H. Cheng, D.Y. Choi, S. Chen, J. Tian, Arbitrary manipulation of light intensity by bilayer aluminum metasurfaces, Adv. Opt. Mater. 7 (2019) 1900260, doi:10.1002/adom.201900260.
[57] J. Li, S. Chen, H. Yang, J. Li, P. Yu, H. Cheng, C. Gu, H.T. Chen, J. Tian, Simultaneous control of light polarization and phase distributions using plasmonic metasurfaces, Adv. Funct. Mater. 25 (2015) 704–710, doi:10.1002/adfm.201403669.
[58] B.O. Raeker, A. Grbic, Compound metaoptics for amplitude and phase control of wave fronts, Phys. Rev. Lett. 122 (2019) 113901, doi:10.1103/PhysRevLett.122.113901.
[59] N.K. Grady, J.E. Heyes, D.R. Chowdhury, Y. Zeng, M.T. Reiten, A.K. Azad, A.J. Taylor, D.A. Dalvit, H.T. Chen, Terahertz metamaterials for linear polarization conversion and anomalous refraction, Science 340 (2013) 1304–1307, doi:10.1126/science.1235399.
[60] Z. Li, S. Chen, W. Liu, H. Cheng, Z. Liu, J. Li, P. Yu, B. Xie, J. Tian, High performance broadband asymmetric polarization conversion due to polarization-dependent reflection, Plasmonics 10 (2015) 1703–1711, doi:10.1007/s11468-015-9986-2.
[61] Z. Li, W. Liu, H. Cheng, J. Liu, S. Chen, J. Tian, Simultaneous generation of high-efficiency broadband asymmetric anomalous refraction and reflection waves with few-layer anisotropic metasurface, Sci. Rep. 6 (2016) 35485, doi:10.1038/srep35485.
[62] W. Luo, S. Sun, H.-X. Xu, Q. He, L. Zhou, Transmissive ultrathin pancharatnam-berry metasurfaces with nearly 100% efficiency, Phys. Rev. Appl. 7 (2017) 044033, doi:10.1103/PhysRevApplied.7.044033.
[63] Z. Li, W. Liu, H. Cheng, D.-Y. Choi, S. Chen, J. Tian, Spin-selective full-dimensional manipulation of optical waves with chiral mirror, Adv. Mater. 32 (2020) 1907983, doi:10.1002/adma.201907983.
[64] F. Monticone, N.M. Estakhri, A. Alù, Full control of nanoscale optical transmission with a composite metascreen, Phys. Rev. Lett. 110 (2013) 203903, doi:10.1103/PhysRevLett.110.203903.
[65] C. Pfeiffer, N.K. Emani, A.M. Shaltout, A. Boltasseva, V.M. Shalaev, A. Grbic, Efficient light bending with isotropic metamaterial huygens' surfaces, Nano Lett. 14 (2014) 2491–2497, doi:10.1021/nl5001746.
[66] J. Liu, Z. Li, W. Liu, H. Cheng, S. Chen, J. Tian, High-efficiency mutual dual-band asymmetric transmission of circularly polarized waves with few-layer anisotropic metasurfaces, Adv. Opt. Mater. 4 (2016) 2028–2034, doi:10.1002/adom.201600602.
[67] Z. Li, W. Liu, C. Tang, H. Cheng, Z. Li, Y. Zhang, J. Li, S. Chen, J. Tian, A. Bilayer, Plasmonic metasurface for polarization-insensitive bidirectional perfect absorption, Adv. Theory Simul. 3 (2020) 1900216, doi:10.1002/adts.201900216.
[68] P. Yu, S. Chen, J. Li, H. Cheng, Z. Li, W. Liu, B. Xie, Z. Liu, J. Tian, Generation of vector beams with arbitrary spatial variation of phase and linear polarization using plasmonic metasurfaces, Opt. Lett. 40 (2015) 3229–3232, doi:10.1364/OL.40.003229.
[69] J. Li, P. Yu, C. Tang, H. Cheng, J. Li, S. Chen, J. Tian, Bidirectional perfect absorber using free substrate plasmonic metasurfaces, Adv. Opt. Mater. 5 (2017) 1700152, doi:10.1002/adom.201700152.
[70] J.P.S. Wong, A. Epstein, G.V. Eleftheriades, Reflectionless wide-angle refracting metasurfaces, IEEE Antennas Wirel. Propag. Lett. 15 (2016) 1293–1296, doi:10.1109/lawp.2015.2505629.
[71] B.O. Raeker, A. Grbic, Lossless complex-valued optical-field control with compound metaoptics, Phys. Rev. Appl. 15 (2021) 054039, doi:10.1103/PhysRevApplied.15.054039.
[72] Raeker, B. O., Zheng, H., Zhou, Y., Kravchenko, I., Valentine, J. & Grbic, A. All-dielectric meta-optics for high-efficiency independent amplitude and phase manipulation. arXiv: Optics (2021).
[73] X. Lin, Y. Rivenson, N.T. Yardimci, M. Veli, Y. Luo, M. Jarrahi, A. Ozcan, All-optical machine learning using diffractive deep neural networks, Science 361 (2018) 1004, doi:10.1126/science.aat8084.
[74] A.S. Backer, Computational inverse design for cascaded systems of metasurface optics, Opt. Expr. 27 (2019) 30308–30331, doi:10.1364/OE.27.030308.
[75] C. Qian, X. Lin, X. Lin, J. Xu, Y. Sun, E. Li, B. Zhang, H. Chen, Performing optical logic operations by a diffractive neural network, Light Sci. Appl. 9 (2020) 59, doi:10.1038/s41377-020-0303-2.
[76] M. Mansouree, H. Kwon, E. Arbabi, A. McClung, A. Faraon, A. Arbabi, Multifunctional 2.5D metastructures enabled by adjoint optimization, Optica 7 (2020) 77–84, doi:10.1364/OPTICA.374787.
[77] Q. Wang, E. Plum, Q. Yang, X. Zhang, Q. Xu, Y. Xu, J. Han, W. Zhang, Reflective chiral meta-holography: multiplexing holograms for circularly polarized waves, Light Sci. Appl. 7 (2018) 25, doi:10.1038/s41377-018-0019-8.
[78] S.D. Rezaei, J. Ho, R.J.H. Ng, S. Ramakrishna, J.K.W. Yang, On the correlation of absorption cross-section with plasmonic color generation, Opt. Express 25 (2017) 27652–27664, doi:10.1364/OE.25.027652.
[79] X. Shen, T.J. Cui, J. Zhao, H.F. Ma, W.X. Jiang, H. Li, Polarization-independent wide-angle triple-band metamaterial absorber, Opt. Express 19 (2011) 9401–9407, doi:10.1364/OE.19.009401.
[80] S. Chen, H. Cheng, H. Yang, J. Li, X. Duan, C. Gu, J. Tian, Polarization insensitive and omnidirectional broadband near perfect planar metamaterial absorber in the near infrared regime, Appl. Phys. Lett. 99 (2011) 253104, doi:10.1063/1.3670333.
[81] B. Wang, F. Dong, Q.T. Li, D. Yang, C. Sun, J. Chen, Z. Song, L. Xu, W. Chu, Y.F. Xiao, Q. Gong, Y. Li, Visible-frequency dielectric metasurfaces for multiwavelength achromatic and highly dispersive holograms, Nano Lett. 16 (2016) 5235–5240, doi:10.1021/acs.nanolett.6b02326.
[82] B. Wang, F. Dong, D. Yang, Z. Song, L. Xu, W. Chu, Q. Gong, Y. Li, Polarization-controlled color-tunable holograms with dielectric metasurfaces, Optica 4 (2017) 1368–1371, doi:10.1364/optica.4.001368.
[83] Y. Bao, Y. Yu, H. Xu, Q. Lin, Y. Wang, J. Li, Z.K. Zhou, X.H. Wang, Coherent pixel design of metasurfaces for multidimensional optical control of multiple printing-image switching and encoding, Adv. Funct. Mater. 28 (2018) 1805306, doi:10.1002/adfm.201805306.
[84] X. Zang, F. Dong, F. Yue, C. Zhang, L. Xu, Z. Song, M. Chen, P.Y. Chen, G.S. Buller, Y. Zhu, S. Zhuang, W. Chu, S. Zhang, X. Chen, Polarization encoded color image embedded in a dielectric metasurface, Adv. Mater. 30 (2018) 1707499, doi:10.1002/adma.201707499.
[85] P. Huo, M. Song, W. Zhu, C. Zhang, L. Chen, H.J. Lezec, Y. Lu, A. Agrawal, T. Xu, Photorealistic full-color nanopainting enabled by low-loss metasurface, Optica 7 (2020) 1171–1172, doi:10.1364/optica.403092.
[86] Z.L. Deng, J. Deng, X. Zhuang, S. Wang, T. Shi, G.P. Wang, Y. Wang, J. Xu, Y. Cao, X. Wang, X. Cheng, G. Li, X. Li, Facile metagrating holograms with broadband and extreme angle tolerance, Light Sci. Appl. 7 (2018) 78, doi:10.1038/s41377-018-0075-0.
[87] P. Yu, J. Li, C. Tang, H. Cheng, Z. Liu, Z. Li, Z. Liu, C. Gu, J. Li, S. Chen, J. Tian, Controllable optical activity with non-chiral plasmonic metasurfaces, Light Sci. Appl. 5 (2016) e16096-e16096., doi:10.1038/lsa.2016.96.
[88] Z. Liu, Z. Li, Z. Liu, H. Cheng, W. Liu, C. Tang, C. Gu, J. Li, H.T. Chen, S. Chen, J. Tian, Single-layer plasmonic metasurface half-wave plates with wavelength-independent polarization conversion angle, Acs Photonics 4 (2017) 2061–2069, doi:10.1021/acsphotonics.7b00491.
[89] Z.L. Deng, J. Deng, X. Zhuang, S. Wang, K. Li, Y. Wang, Y. Chi, X. Ye, J. Xu, G.P. Wang, R. Zhao, X. Wang, Y. Cao, X. Cheng, G. Li, X. Li, Diatomic metasurface for vectorial holography, Nano Lett. 18 (2018) 2885–2892, doi:10.1021/acs.nanolett.8b00047.
[90] Q. Song, S. Khadir, S. Vézian, B. Damilano, P.D. Mierry, S. Chenot, V. Brandli, P. Genevet, Bandwidth-unlimited polarization-maintaining metasurfaces, Sci. Adv. 7 (2021) eabe1112, doi:10.1126/sciadv.abe1112.
[91] Z.L. Deng, M. Jin, X. Ye, S. Wang, T. Shi, J. Deng, N. Mao, Y. Cao, B.O. Guan, A. Alù, G. Li, X. Li, Full-color complex-amplitude vectorial holograms based on multi-freedom metasurfaces, Adv. Funct. Mater. 30 (2020), doi:10.1002/adfm.201910610.
[92] S. Gao, C.S. Park, C. Zhou, S.S. Lee, D.Y. Choi, Twofold polarization-selective all-dielectric trifoci metalens for linearly polarized visible light, Adv. Opt. Mater. 7 (2019) 1900883, doi:10.1002/adom.201900883.

[93] Y. Bao, J. Ni, C.W. Qiu, A minimalist single-layer metasurface for arbitrary and full control of vector vortex beams, Adv. Mater. 32 (2020) 1905659, doi:10.1002/adma.201905659.
[94] X. Duan, S. Chen, H. Yang, H. Cheng, J. Li, W. Liu, C. Gu, J. Tian, Polarization-insensitive and wide-angle plasmonically induced transparency by planar metamaterials, Appl. Phys. Lett. 101 (2012) 143105, doi:10.1063/1.4756944.
[95] X. Duan, S. Chen, H. Cheng, Z. Li, J Tian, Dynamically tunable plasmonically induced transparency by planar hybrid metamaterial, Opt. Lett. 38 (2013) 483–485, doi:10.1364/OL.38.000483.
[96] S. Gao, C. Zhou, W. Yue, Y. Li, C. Zhang, H. Kan, C. Li, S.S. Lee, D.Y. Choi, Efficient all-dielectric diatomic metasurface for linear polarization generation and 1-bit phase control, ACS Appl. Mater. Interfaces 13 (2021) 14497–14506, doi:10.1021/acsami.1c00967.
[97] Z. Liu, Z. Li, Z. Liu, J. Li, H. Cheng, P. Yu, W. Liu, C. Tang, C. Gu, J. Li, S. Chen, J. Tian, High-performance broadband circularly polarized beam deflector by mirror effect of multinanorod metasurfaces, Adv. Funct. Mater. 25 (2015) 5428–5434, doi:10.1002/adfm.201502046.
[98] T. Shi, Z.-L. Deng, Q.-A. Tu, Y. Cao, X. Li, Displacement-mediated bound states in the continuum in all-dielectric superlattice metasurfaces, PhotoniX 2 (2021), doi:10.1186/s43074-021-00029-x.
[99] A. Tittl, A. Leitis, M. Liu, F. Yesilkoy, D.-Y. Choi, D.N. Neshev, Y.S. Kivshar, H. Altug, Imaging-based molecular barcoding with pixelated dielectric metasurfaces, Science 360 (2018) 1105, doi:10.1126/science.aas9768.
[100] M. Kenney, S. Li, X. Zhang, X. Su, T.T. Kim, D. Wang, D. Wu, C. Ouyang, J. Han, W. Zhang, H. Sun, S. Zhang, Pancharatnam-berry phase induced spin-selective transmission in herringbone dielectric metamaterials, Adv. Mater. 28 (2016) 9567–9572, doi:10.1002/adma.201603460.
[101] F. Zhang, M. Pu, X. Li, P. Gao, X. Ma, J. Luo, H. Yu, X. Luo, All-dielectric metasurfaces for simultaneous giant circular asymmetric transmission and wavefront shaping based on asymmetric photonic spin-orbit interactions, Adv. Funct. Mater. 27 (2017) 1704295, doi:10.1002/adfm.201704295.
[102] D. Ma, Z. Li, Y. Zhang, W. Liu, H. Cheng, S. Chen, J. Tian, Giant spin-selective asymmetric transmission in multipolar-modulated metasurfaces, Opt. Lett. 44 (2019) 3805–3808, doi:10.1364/OL.44.003805.
[103] S. Wang, Z.L. Deng, Y. Wang, Q. Zhou, X. Wang, Y. Cao, B.O. Guan, S. Xiao, X. Li, Arbitrary polarization conversion dichroism metasurfaces for all-in-one full Poincare sphere polarizers, Light Sci. Appl. 10 (2021) 24, doi:10.1038/s41377-021-00468-y.
[104] J. Cai, F. Zhang, M. Zhang, Y. Ou, H. Yu, Simultaneous polarization filtering and wavefront shaping enabled by localized polarization-selective interference, Sci. Rep. 10 (2020) 14477, doi:10.1038/s41598-020-71508-7.
[105] Y. Huang, T. Xiao, Z. Xie, J. Zheng, Y. Su, W. Chen, K. Liu, M. Tang, P. Müller-Buschbaum, L. Li, Single-layered reflective metasurface achieving simultaneous spin-selective perfect absorption and efficient wavefront manipulation, Adv. Opt. Mater. 9 (2020) 2001663, doi:10.1002/adom.202001663.
[106] A.S. Rana, I. Kim, M.A. Ansari, M.S. Anwar, M. Saleem, T. Tauqeer, A. Danner, M. Zubair, M.Q. Mehmood, J. Rho, Planar achiral metasurfaces-induced anomalous chiroptical effect of optical spin isolation, ACS Appl. Mater. Interfaces 12 (2020) 48899–48909, doi:10.1021/acsami.0c10006.
[107] Y. Bao, Y. Yu, H. Xu, C. Guo, J. Li, S. Sun, Z.K. Zhou, C.W. Qiu, X.H. Wang, Full-colour nanoprint-hologram synchronous metasurface with arbitrary hue-saturation-brightness control, Light Sci. Appl. 8 (2019) 95, doi:10.1038/s41377-019-0206-2.
[108] Q. Fan, M. Liu, C. Zhang, W. Zhu, Y. Wang, P. Lin, F. Yan, L. Chen, H.J. Lezec, Y. Lu, A. Agrawal, T. Xu, Independent amplitude control of arbitrary orthogonal states of polarization via dielectric metasurfaces, Phys. Rev. Lett. 125 (2020) 267402, doi:10.1103/PhysRevLett.125.267402.
[109] Y. Bao, L. Wen, Q. Chen, C.W. Qiu, B. Li, Toward the capacity limit of 2D planar Jones matrix with a single-layer metasurface, Sci. Adv. 7 (2021) eabh0365, doi:10.1126/sciadv.abh0365.
[110] M. Liu, W. Zhu, P. Huo, L. Feng, M. Song, C. Zhang, L. Chen, H.J. Lezec, Y. Lu, A. Agrawal, T. Xu, Multifunctional metasurfaces enabled by simultaneous and independent control of phase and amplitude for orthogonal polarization states, Light Sci. Appl. 10 (2021) 107, doi:10.1038/s41377-021-00552-3.
[111] Z. Li, W. Liu, H. Cheng, S. Chen, J. Tian, Spin-selective transmission and devisable chirality in two-layer metasurfaces, Sci. Rep. 7 (2017) 8204, doi:10.1038/s41598-017-08527-4.
[112] K. Tanaka, D. Arslan, S. Fasold, M. Steinert, J. Sautter, M. Falkner, T. Pertsch, M. Decker, I. Staude, Chiral bilayer all-dielectric metasurfaces, ACS Nano 14 (2020) 15926–15935, doi:10.1021/acsnano.0c07295.
[113] A. Overvig, N. Yu, A. Alu, Chiral quasi-bound states in the continuum, Phys. Rev. Lett. 126 (2021) 073001, doi:10.1103/PhysRevLett.126.073001.
[114] D. Frese, Q. Wei, Y. Wang, L. Huang, T. Zentgraf, Nonreciprocal asymmetric polarization encryption by layered plasmonic metasurfaces, Nano Lett. 19 (2019) 3976–3980, doi:10.1021/acs.nanolett.9b01298.
[115] C. Zhang, G. Wang, H.X. Xu, X. Zhang, H.P. Li, Helicity-dependent multifunctional metasurfaces for full-space wave control, Adv. Opt. Mater. 8 (2020) 1901719, doi:10.1002/adom.201901719.
[116] A.M. Shaltout, V.M. Shalaev, M.L. Brongersma, Spatiotemporal light control with active metasurfaces, Science 364 (2019) eaat3100, doi:10.1126/science.aat3100.
[117] Q. He, S. Sun, L. Zhou, Tunable/reconfigurable metasurfaces: physics and applications, Research 2019 (2019) 1849272 (Wash D C), doi:10.34133/2019/1849272.
[118] J. Li, S. Kamin, G. Zheng, F. Neubrech, S. Zhang, N. Liu, Addressable metasurfaces for dynamic holography and optical information encryption, Sci. Adv. 4 (2018) eaar6768, doi:10.1126/sciadv.aar6768.
[119] Z. Wu, Y. Ra'di, A Grbic, Tunable metasurfaces: a polarization rotator design, Phys. Rev. X 9 (2019) 011036, doi:10.1103/PhysRevX.9.011036.
[120] F. Walter, G. Li, C. Meier, S. Zhang, T. Zentgraf, Ultrathin nonlinear metasurface for optical image encoding, Nano Lett. 17 (2017) 3171–3175, doi:10.1021/acs.nanolett.7b00676.
[121] N. Mao, J. Deng, X. Zhang, Y. Tang, M. Jin, Y. Li, X. Liu, K. Li, T. Cao, K. Cheah, H. Wang, J. Ng, G. Li, Nonlinear diatomic metasurface for real and fourier space image encoding, Nano Lett. 20 (2020) 7463–7468, doi:10.1021/acs.nanolett.0c02910.
[122] Y. Liang, H. Lin, K. Koshelev, F. Zhang, Y. Yang, J. Wu, Y. Kivshar, B. Jia, Full-stokes polarization perfect absorption with diatomic metasurfaces, Nano Lett. 21 (2021) 1090–1095, doi:10.1021/acs.nanolett.0c04456.
[123] J. Lin, M. Qiu, X. Zhang, H. Guo, Q. Cai, S. Xiao, Q. He, L. Zhou, Tailoring the lineshapes of coupled plasmonic systems based on a theory derived from first principles, Light Sci. Appl. 9 (2020) 158, doi:10.1038/s41377-020-00386-5.